Preplanned Studies

Epidemiological Assessment and Optimization of School-Based Influenza Vaccination — Shenzhen City, Guangdong Province, China, 2023–2024

Shuqi Wang^{1,2,3,&}; Zhigao Chen^{4,&}; Qi Tan⁵; Zengyang Shao^{1,3}; Yushuang Chen^{1,3}; Fang Huang⁴; Yanpeng Cheng⁴; Jianxing Yu⁶; Ting Zhang⁶; Xin Wang⁴; Xiujuan Tang^{4,#}; Zhen Zhang⁴; Chao Gao^{7,#}; Zhongjie Li^{6,#}; Zhanwei Du^{8,9}

Summary

What is already known about this topic?

School-aged children represent a particularly vulnerable population for influenza transmission due to their dense social interactions and limited awareness of protective measures. Since 2019, Shenzhen has provided free influenza immunizations to this demographic, with vaccination campaigns typically initiated during the autumn months.

What is added by this report?

This study utilized influenza surveillance data from Shenzhen to develop an age-stratified compartmental model for epidemiological simulations, evaluating the disease burden prevented by influenza vaccinations among school-aged children during the 2023–2024 season. Additionally, an optimization framework was developed to design strategic vaccination schedules while considering the importance of maintaining stable public health policies over time.

What are the implications for public health practice?

The findings suggest concentrating vaccination efforts during November and December; however, optimal strategies may vary depending on specific influenza transmission patterns. A more robust approach involves implementing a generalized strategy optimized using historical seasonal data with comparable transmission characteristics.

ABSTRACT

Introduction: School-aged children are primary vectors for influenza transmission through their frequent close contact in educational settings and developing immune awareness. Since 2019, the Shenzhen municipal government has implemented annual, free, influenza vaccination programs targeting

eligible primary and secondary school students. However, evidence-based strategies specifically tailored to this demographic remain insufficient.

Methods: This study analyzed weekly influenza-like illness (ILI) surveillance data and laboratory-confirmed positivity rates from Shenzhen during the 2023–2024 season. It developed an age-stratified Susceptible—Exposed—Symptomatic—Asymptomatic—Recovered—Hospitalized—Deceased—Vaccinated compartmental model integrated with the Ensemble Adjustment Kalman Filter (EAKF) algorithm to estimate historical transmission parameters and quantify vaccination impact. The Upper Confidence Bound applied to Trees (UCT) algorithm was used to optimize the vaccination schedule and evaluate multiple strategic scenarios comparatively.

Results: Compared to a no-vaccination scenario, the current government strategy prevented approximately 1,285,925 [95% confidence interval 1,240,671-1,331,180] symptomatic infections and 56,956 (95% *CI*: 55,118–58,793) hospitalizations. Under identical vaccine supply conditions, the optimized strategy recommends vaccinating 30%, 25%, and 5% of school-aged children in November, December, and January, respectively. This optimized approach would avert approximately 1,469,368 (95% CI: 1,392,734–1,546,002) symptomatic infections and 64,442 (95% CI: 61,269-67,615) hospitalizations representing 14.3% and 13.1% improvements over the government strategy, respectively. Additionally, a generic strategy developed using 2017-2019 data performed well during 2023-2024, demonstrating cross-seasonal adaptability.

Conclusions: Concentrating influenza vaccination efforts among school-enrolled children during November and December significantly reduces disease burden and represents a critical strategy for controlling influenza transmission.

Influenza represents a significant acute respiratory infectious disease that poses substantial public health worldwide. Educational institutions, characterized by dense student populations, limited mobility patterns, and frequent close interpersonal contact, constitute particularly high-risk environments for influenza transmission and outbreaks (1). Schoolaged children demonstrate heightened susceptibility to viral infection compared to adults and, once infected, typically exhibit prolonged viral shedding periods with higher viral loads (2). These epidemiological characteristics underscore the critical importance of implementing targeted, evidence-based countermeasures within school settings. Among available pharmaceutical interventions, vaccination remains the most effective strategy for preventing influenza-related infections (3).

Since 2019, Shenzhen's vaccination program has provided free influenza vaccinations to school-aged typically implementing these programs during October and November each year. Despite influenza extensive research vaccination on optimization strategies (4-5), the evidence base supporting vaccination decisions for this specific population remains limited, creating a gap between recommendations theoretical and practical implementation for school-based programs.

To assess the epidemiological impact of school-based vaccination programs, this study analyzed influenza transmission patterns in Shenzhen during the 2023-2024 season and compared observed outcomes with simulated scenarios assuming no vaccination intervention. This study utilized weekly ILI+ proxy data spanning August 2023 to July 2024, along with vaccination coverage data provided by the Shenzhen Center for Disease Control and Prevention (CDC), to estimate reductions in infections and hospitalizations attributable to vaccination (Supplementary Material and Supplementary Figure S1, available at https:// weekly.chinacdc.cn/). The ILI+ proxy integrates influenza-like illness (ILI) rates with laboratoryconfirmed positivity rates, providing a comprehensive measure of influenza activity that captures both clinical presentation and virological confirmation. reconstruct historical influenza transmission dynamics, this study implemented an age-specific Susceptible -Exposed – Symptomatic – Asymptomatic – Recovered – Hospitalized – Deceased – Vaccinated (SEYARHDV) compartmental model, which effectively characterizes viral spread across different population segments (Supplementary Material, Supplementary Figure S2,

and Supplementary Table S1, available at https:// weekly.chinacdc.cn/). By coupling this transmission model with the Ensemble Adjustment Kalman Filter (EAKF) algorithm (6), this study estimated timevarying transmission rates and other epidemiological parameters to quantify the public health impact of vaccination programs, specifically measuring reductions in symptomatic infections and hospitalizations (Supplementary Material).

For the optimization process, this study employed the Upper Confidence Bound applied to Trees (UCT) algorithm to identify an optimal vaccination schedule for school-aged children (Supplementary Material) (7). To address implementation challenges such as dispersed vaccination timing and uneven distribution patterns, it introduced a smoothness constraint to ensure gradual policy rollout and prevent abrupt strategic shifts. The optimization framework begins each September — coinciding with the academic year commencement — and spans a 12-month period with monthly decision intervals, aiming to minimize annual influenza-related hospitalizations. Based on the vaccination strategy implemented by the Shenzhen government, as documented by the Shenzhen CDC for 2023-2024, this study established an annual vaccination rate of 60% for children aged 6-18 years. Each month offers 6 vaccination options: 0%, 5%, 10%, 25%, 30%, or 45%, permitting up to 45% of school-aged children to receive vaccination monthly. For other age groups (0–5 years, 19–59 years, and \geq 60 years), monthly and annual vaccination rates align with actual vaccination data from 2023 to 2024. Under the baseline strategy — where annual vaccination rates are distributed evenly across months — school-aged children receive a consistent monthly vaccination rate of 5%, while other groups maintain their default Vaccines are administered throughout each day. Additional experimental details are provided in Supplementary Material.

For the 2023–2024 period, this study fitted the SEYARHDV model and found that the influenza season extended from September 2023 to May 2024, with a peak ILI+ proxy of 0.0665 (Figure 1A). In a simulated scenario without vaccination, the projected peak ILI+ proxy increased dramatically to 0.2728, demonstrating the critical importance of vaccination in epidemic control. The Shenzhen vaccination program prevented approximately 1,285,925 (95% *CI*: 1,240,671–1,331,180) symptomatic infections and 56,956 (95% *CI*: 55,118–58,793) hospitalizations in 2023–2024. By comparison, the baseline vaccination

strategy prevented only 704,669 (95% CI: 669,089-740,249) symptomatic infections and 32,175 30,641–33,709) hospitalizations, demonstrating substantially lower effectiveness than the government's approach. Using the same vaccine supply, optimized strategy recommended vaccinating 30%, 25%, and 5% of school-aged children in November, December, and January, respectively. This optimized approach could prevent 1,469,368 (95% CI: 1,392,734–1,546,002) symptomatic infections and 64,442 (95% CI: 61,269-67,615) hospitalizations. Compared to the government's vaccination strategy, the optimized approach achieved a 14.3% greater reduction in symptomatic infections and a 13.1% greater reduction in hospitalizations, demonstrating superior effectiveness in controlling influenza transmission.

Figure 1B illustrates the differences in ILI+ proxy trends across vaccination strategies. Similar analyses were conducted using 2017–2019 data, with results provided in Supplementary Material and Supplementary Figure S3 (available at https://weekly.chinacdc.cn/).

To develop a vaccination strategy applicable to future influenza seasons, this study sought to derive an optimal approach using historical data that could be applied to prospective scenarios. It optimized vaccination strategies for the 2017–2018 and 2018–2019 influenza seasons using data from 2017 to 2019 (Supplementary Material). A comprehensive, universal strategy was obtained by calculating a weighted average of the optimization results from these two seasons, which recommended vaccinating 15% and 45% of school-aged children in October and

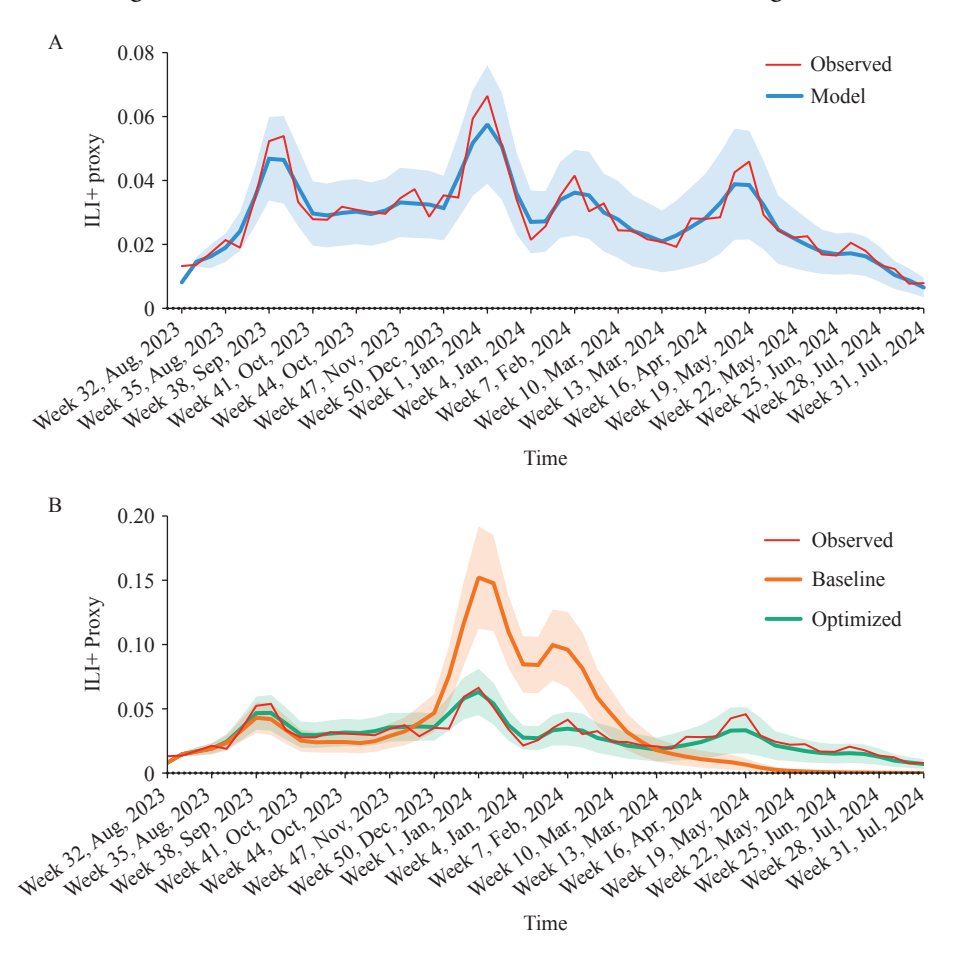


FIGURE 1. Model fitting and simulation of influenza activity under different vaccination strategies, Shenzhen, 2023–2024. (A) Observed ILI+ proxy from surveillance data (red) and corresponding model fitting results (blue line with shaded 95% *CI*). (B) Comparison of observed ILI+ (red) with model-simulated outcomes under two strategies: baseline (orange) and optimized (green), shown as lines with shaded 95% *CI*s.

Note: All scenarios assume the same annual vaccine coverage. For school-aged children, only the monthly distribution differs; other age groups follow actual 2023–2024 rates.

Abbreviation: C/=confidence interval; ILI+=influenza-positive proportion.

November, respectively. When this strategy was applied to the 2023–2024 influenza season, it potentially reduced symptomatic infections 1,187,407 (95% CI: 1,150,194-1,224,620) and hospitalizations by 52,924 (95% CI: 51,408-54,439). Although this strategy's effectiveness was slightly lower than the government-enforced strategy, demonstrated robust performance, making it suitable vaccination policy recommendations. difference in effectiveness can be attributed to significant variations in transmission patterns across different influenza seasons. For instance, 2017–2018 influenza season was predominantly confined to the winter-spring period with relatively low case numbers, while the 2018-2019 experienced significant outbreaks in both winter-spring and summer periods. In contrast, the 2023-2024 season extended from summer and autumn to the following spring and summer, with a higher overall peak. These findings suggest that future strategy optimization should incorporate more comprehensive historical data and predictions about influenza transmission levels. A universal strategy optimized using data from seasons with similar transmission patterns would likely prove more effective and better suited to adapting to the dynamic nature of influenza transmission.

To better understand how different age groups contribute to the observed vaccination effectiveness, this study conducted additional simulations by sequentially removing vaccination coverage for each age group while maintaining coverage for all others. This approach allowed the quantification of the marginal impact of each age group on overall disease burden during the 2023-2024 season. The results demonstrated that removing vaccination for the 6-18 year group led to the most substantial increase in disease burden, resulting in an estimated 3,823,546 (95% CI: 3,513,522–4,133,570) symptomatic infections and 175,283 (95% CI: 162,422-188,143) hospitalizations — substantially higher than any other age group. In comparison, removing vaccination for the 0-5 year group resulted in 2,679,188 (95% CI: 2,406,184-2,952,192) symptomatic infections and 128,517 (95% CI: 116,848-140,186) hospitalizations. Removing vaccination for the 19-59 year group yielded 2,719,808 (95% CI: 2,444,489-2,995,128) symptomatic infections and 130,408 (95% CI: 118,631-142,185) hospitalizations. Finally, removing vaccination for the ≥60 year group led to 2,677,089 2,404,110–2,950,069) (95% CI: symptomatic infections and 130,414 (95% CI: 118,546–142,282) hospitalizations. These findings highlight that while all age groups contribute to overall protection, the marginal impact of vaccinating school-aged children is notably greater in reducing population-level transmission and disease burden. This result aligns with both theoretical expectations and practical implementation, as the Shenzhen vaccination program has primarily targeted school-aged children and achieved the highest coverage in this demographic.

DISCUSSION

The spread of influenza has created severe health school-aged challenges among children. This demographic faces heightened susceptibility to crossinfection within school environments due to their limited self-protection awareness and frequent close peer interactions (8). Such intensive contact not only facilitates within-school transmission but significantly amplifies community-level spread. Infected children often serve as vectors, carrying the virus into their households and triggering cascading consequences, including parental absenteeism and secondary infections among family members. Research demonstrates that for every 10 students absent from school due to influenza, approximately 8 household members subsequently become ill, with illness rates within 3 days of school absence being 2.2 times higher than expected during the influenza season (9). This evidence confirms that school-aged children frequently serve as primary introducers of influenza into households. Consequently, vaccinating school-aged children not only reduces their individual disease burden but also disrupts transmission pathways between schools and households, helping to curb thereby community-level spread and broader alleviating the overall public health and socioeconomic burden of seasonal influenza.

Although school-aged children are not traditionally considered the primary target of influenza vaccination, many countries now recommend including them in immunization programs as an extension of existing plans (10). This shift reflects growing recognition of their central role in influenza transmission. In Shenzhen, influenza vaccination is available to all individuals aged 6 months and older, with free vaccinations currently accessible only to school-aged children and elderly individuals aged 60 and above. Others who intend to receive vaccinations need to voluntarily visit clinics at their own expense for

preventive immunization. It is worth noting that influenza vaccination for the elderly is also entirely voluntary. Hence, this study investigated the public health benefits of vaccination policies and examined optimal strategies for vaccinating school-aged children. Its findings underscore the importance of vaccination timing and coverage, highlighting the advantages of well-planned public health interventions.

This study has several limitations that should be acknowledged. First, its investigation of vaccination strategies did not consider other interventions such as social distancing measures. Second, this study utilized weekly ILI+ proxy data and healthcare-seeking rates to estimate symptomatic incidence in the general population from municipal-scale data, which may introduce biases in attack rate calculations. Third, this study considered only six possible vaccination actions to balance varying vaccination rates while minimizing computational complexity. It also assumed a maximum monthly vaccination rate of 45%, which constrained this study's action space. Regions can adjust these actions and constraints based on their vaccination capacity and local conditions. Fourth, since unified mass influenza vaccination targets only school-aged children, this study assumed vaccination rates for other age groups remained fixed and focused solely on optimizing the vaccination schedule for school-aged children. However, this methodology can be similarly applied to other regions and age groups.

This study's findings demonstrate that Shenzhen's large-scale, targeted vaccination program for schoolaged children substantially reduces influenza-related disease burden, including both infections and hospitalizations. The optimization algorithm that this study developed provides a valuable framework for refining vaccination strategies across different settings. While vaccination approaches may require adaptation specific influenza transmission patterns, concentrating vaccination efforts during November December consistently proves effective, establishing a robust foundation for future vaccination policies.

Conflicts of interest: No conflicts of interest.

Funding: Supported by the National Key R&D Program of China (2022YFE0112300, 2023YFC2308701), the National Natural Science Foundation of China (82304204), the Natural Science Foundation of Guangdong Province (2025A1515011908), the Technological Innovation Team of Shaanxi Province (2025RS-CXTD-009), the

International Cooperation Project of Shaanxi Province (2025GH-YBXM-017), the Shenzhen-Hong Kong-Macau Science and Technology Project (Category C) (SGDX20230821091559022), the Fundamental Research Funds for the Central Universities (G2024WD0151, D5000240309), and the CAMS Innovation Fund for Medical Sciences (2021-I2M-1-044).

doi: 10.46234/ccdcw2025.232

Copyright © 2025 by Chinese Center for Disease Control and Prevention. All content is distributed under a Creative Commons Attribution Non Commercial License 4.0 (CC BY-NC).

Submitted: July 21, 2025 Accepted: September 25, 2025 Issued: October 31, 2025

REFERENCES

- Shi JH, Xiang NJ, Zhang YP, Chen M, Sun SH, Chen T, et al. Epidemiological characteristics on the clustering nature of pandemic (H1N1) 2009 in China. Chin J Epidemiol 2012;33(1):62 – 6. https://doi.org/10.3760/cma.j.issn.0254-6450.2012.01.014.
- Wu S, Van Asten L, Wang L, McDonald SA, Pan Y, Duan W, et al. Estimated incidence and number of outpatient visits for seasonal influenza in 2015-2016 in Beijing, China. Epidemiol Infect 2017;145 (16):3334 – 44. https://doi.org/10.1017/S0950268817002369.
- 3. Wang Z, Bauch CT, Bhattacharyya S, d'Onofrio A, Manfredi P, Perc M, et al. Statistical physics of vaccination. Phys Rep 2016;664:1 113. https://doi.org/10.1016/j.physrep.2016.10.006.
- Venkatramanan S, Chen JZ, Fadikar A, Gupta S, Higdon D, Lewis B, et al. Optimizing spatial allocation of seasonal influenza vaccine under temporal constraints. PLoS Comput Biol 2019;15(9):e1007111. https://doi.org/10.1371/journal.pcbi.1007111.
- Kahana D, Yamin D. Accounting for the spread of vaccination behavior to optimize influenza vaccination programs. PLoS One 2021;16(6): e0252510. https://doi.org/10.1371/journal.pone.0252510.
- 6. Pei S, Teng X, Lewis P, Shaman J. Optimizing respiratory virus surveillance networks using uncertainty propagation. Nat Commun

^{*} Corresponding authors: Xiujuan Tang, txj43@126.com; Chao Gao, cgao@nwpu.edu.cn; Zhongjie Li, lizhongjie@sph.pumc.edu.cn.

WHO Collaborating Centre for Infectious Disease Epidemiology and Control, School of Public Health, Li Ka Shing Faculty of Medicine, University of Hong Kong, Hong Kong Special Administrative Region, ² School of Cybersecurity, Northwestern Polytechnical University, Xi'an City, Shaanxi Province, China; 3 Laboratory of Data Discovery for Health Limited, Hong Kong Science and Technology Park, Hong Kong Special Administrative Region, China; ⁴ Shenzhen Center for Disease Control and Prevention, Shenzhen City, Guangdong Province, China; 5 College of Computer and Information Engineering (College of Artificial Intelligence), Nanjing Tech University, Nanjing City, Jiangsu Province, China; 6 School of Population Medicine and Public Health, Chinese Academy of Medical Sciences & Peking Union Medical College, Beijing, China; School of Artificial Intelligence, Optics, and Electronics (iOPEN), Northwestern Polytechnical University, Xi'an City, Shaanxi Province, China; 8 School of Public Health and Emergency Management, Southern University of Science and Technology, Shenzhen City, Guangdong Province, China; ⁹ School of Medicine, Yunnan University, Kunming City, Yunnan Province, China. & Joint first authors.

China CDC Weekly

- 2021;12(1):222. https://doi.org/10.1038/s41467-020-20399-3.
- Kocsis L, Szepesvári C. Bandit based monte-carlo planning. In: Proceedings of the 17th European conference on machine learning. Berlin, Germany: Springer. 2006; p. 282-93. http://dx.doi.org/10. 1007/11871842_29.
- Uscher-Pines L, Schwartz HL, Ahmed F, Zheteyeva Y, Tamargo Leschitz J, Pillemer F, et al. Feasibility of social distancing practices in US schools to reduce influenza transmission during a pandemic. J Public Health Manag Pract 2020;26(4):357 – 70. https://doi.org/10.
- 1097/PHH.000000000001174.
- Neuzil KM, Hohlbein C, Zhu YW. Illness among schoolchildren during influenza season: effect on school absenteeism, parental absenteeism from work, and secondary illness in families. Arch Pediatr Adolesc Med 2002;156(10):986 – 91. https://doi.org/10.1001/ archpedi.156.10.986.
- Newall AT, Jit M, Beutels P. Economic evaluations of childhood influenza vaccination: a critical review. Pharmacoeconomics 2012;30 (8):647 – 60. https://doi.org/10.2165/11599130-0000000000-00000.

SUPPLEMENTARY MATERIAL

Data Description

The Shenzhen Center for Disease Control and Prevention provided influenza-like illness (ILI) rates and laboratory-confirmed positivity rates for Shenzhen across 2 distinct periods: Week 45 of 2017 to Week 44 of 2019, preceding the implementation of large-scale centralized vaccination policies for school-aged children, and Week 32 of 2023 to Week 31 of 2024, following policy implementation (Supplementary Figure S1). Data from 2019 to 2023 were excluded to eliminate potential confounding effects from the coronavirus disease 2019 pandemic. ILI encompasses patients presenting with acute respiratory infection, fever (≥38 °C), cough, and/or sore throat. The ILI+ proxy represents the proportion of influenza-positive cases among individuals seeking medical care, calculated by multiplying the ILI rate (ILI%) by the laboratory-positive rate. Influenza season onset is identified as the initial period of 3 consecutive weeks during which ILI+ records exceed a specified baseline, defined as the 40th percentile of non-zero ILI+ records. The season concludes when 2 consecutive weeks show ILI+ records falling below this baseline following onset. To exclude transient spikes, only periods where ILI+ records consistently exceed 3 times the baseline are considered part of the influenza season (1).

This study assumed a parameter μ to map weekly ILI+ proxy values to weekly symptomatic incidence rates in the general population. To determine the optimal μ value, we selected values in 0.05 increments within the 0 to 1 range. The optimal μ value was identified by minimizing the mean squared error (MSE) between simulated and observed ILI+ proxy means.

Epidemic Influenza Transmission Model

This study employed an age-specific Susceptible – Exposed – Symptomatic – Asymptomatic – Recovered – Hospitalized – Deceased (SEYARHD) model to conduct retrospective forecasts of multiple influenza seasons (Supplementary Figure S2A). To explore optimal vaccination strategies, we incorporated a Vaccinated state into the model (Supplementary Figure S2B), resulting in the SEYARHDV model with the following equations:

$$S_{t+1,a} = S_{t,a} - \beta_t S_{t,a} \sum_{i=1}^{4} \left(Y_{t,i} + \omega A_{t,i} \right) \varphi_{ai} / \psi_a + p^{RS} R_{t,a} - u_{t,a} \psi_a S_{t,a} / \left(S_{t,a} + A_{t,a} \right) + f^b V_{t,a}^b$$

$$E_{t+1,a} = E_{t,a} + \beta_t S_{t,a} \sum_{i=1}^{4} \left(Y_{t,i} + \omega A_{t,i} \right) \varphi_{ai} / \psi_a - p^{EYA} E_{t,a} + \beta_t \sum_{j=1}^{6} \left(1 - v^j \right) V_{t,a}^j \sum_{i=1}^{4} \left(Y_{t,i} + \omega A_{t,i} \right) \varphi_{ai} / \psi_a$$

$$Y_{t+1,a} = Y_{t,a} + \sigma p^{EYA} E_{t,a} - p^{YH} Y_{t,a} - p^{YR} Y_{t,a}$$

$$A_{t+1,a} = A_{t,a} + \left(1 - \sigma \right) p^{EYA} E_{t,a} - p^{AR} A_{t,a}$$

$$R_{t+1,a} = R_{t,a} + p^{AR} A_{t,a} + p^{YR} Y_{t,a} + p^{HR} H_{t,a} - p^{RS} R_{t,a}$$

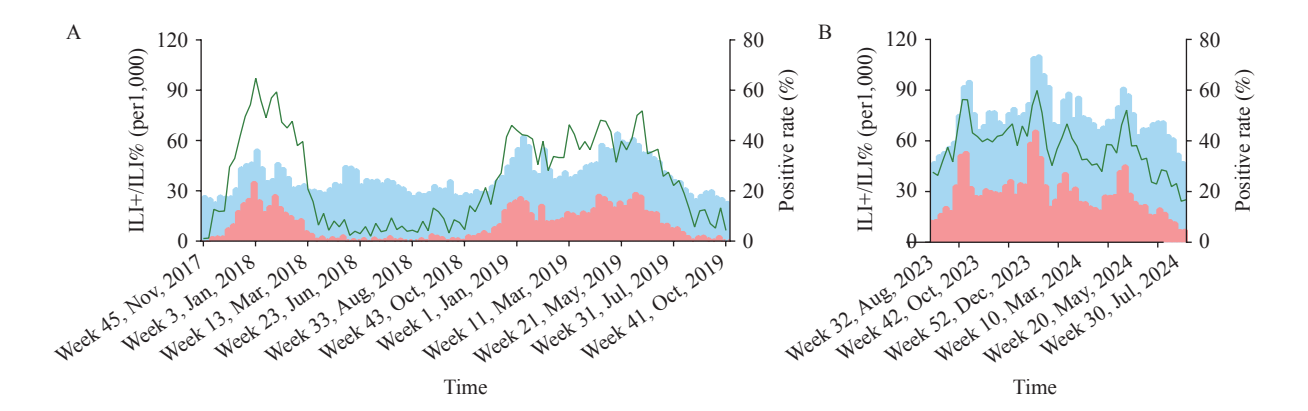
$$H_{t+1,a} = H_{t,a} + p^{YH} Y_{t,a} - p^{HR} H_{t,a} - p^{HD} H_{t,a}$$

$$V_{t+1,a}^1 = V_{t,a}^1 + u_{t,a} \psi_a S_{t,a} / \left(S_{t,a} + A_{t,a} \right) - f^b V_{t,a}^1 - \beta_t \left(1 - v^b \right) V_{t,a}^1 \sum_{i=1}^{4} \left(Y_{t,i} + \omega A_{t,i} \right) \varphi_{ai} / \psi_a, \quad k = 2, 3, 4, 5$$

$$V_{t+1,a}^k = V_{t,a}^k + f^{k-1} V_{t,a}^{k-1} - f^k V_{t,a}^k - \beta_t \left(1 - v^b \right) V_{t,a}^k \sum_{i=1}^{4} \left(Y_{t,i} + \omega A_{t,i} \right) \varphi_{ai} / \psi_a, \quad k = 2, 3, 4, 5$$

$$V_{t+1,a}^k = V_{t,a}^k + f^k V_{t,a}^k - f^k V_{t,a}^k - \beta_t \left(1 - v^b \right) V_{t,a}^k \sum_{i=1}^{4} \left(Y_{t,i} + \omega A_{t,i} \right) \varphi_{ai} / \psi_a$$

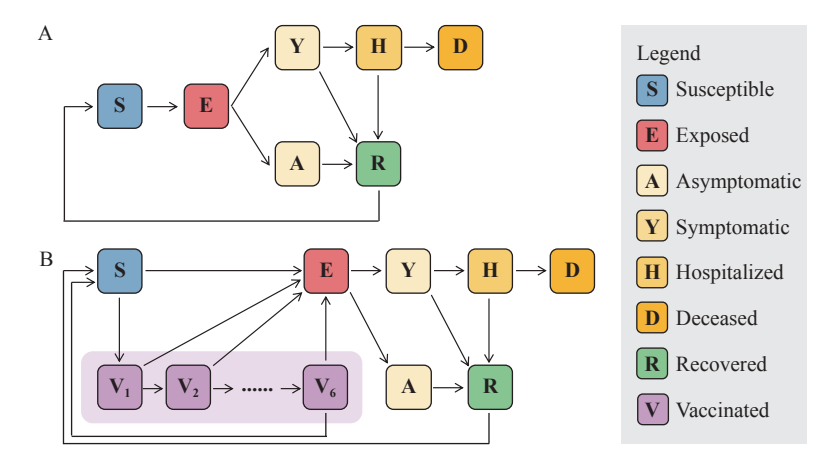
where t represents the time step and a represents age groups (a = 1, 2, 3, 4). S, E, Y, A, R, H, D, and V denote the proportions of the population that are susceptible, exposed, symptomatic infected, asymptomatic infected, recovered, hospitalized, deceased, and vaccinated, respectively. To capture the rise in vaccine efficacy at 1 month followed by a decline at 6 months post-vaccination (2), V is divided into 6 sub-compartments, each with a vaccine efficacy v^k and transition rates between sub-compartments f^k (k = 1, 2, ..., 6). Since asymptomatic individuals exhibit



SUPPLEMENTARY FIGURE S1. Weekly trends of ILI%, laboratory-confirmed positivity rate, and the calculated ILI+ proxy in Shenzhen from (A) 2017 to 2019 and (B) 2023 to 2024.

Note: The red-shaded area represents the ILI+ proxy, the blue-shaded area represents ILI%, and the green curve indicates the laboratory-confirmed positivity rate.

Abbreviation: ILI=influenza-like illness; ILI%=influenza-like illness rate; ILI+=influenza-positive proportion.

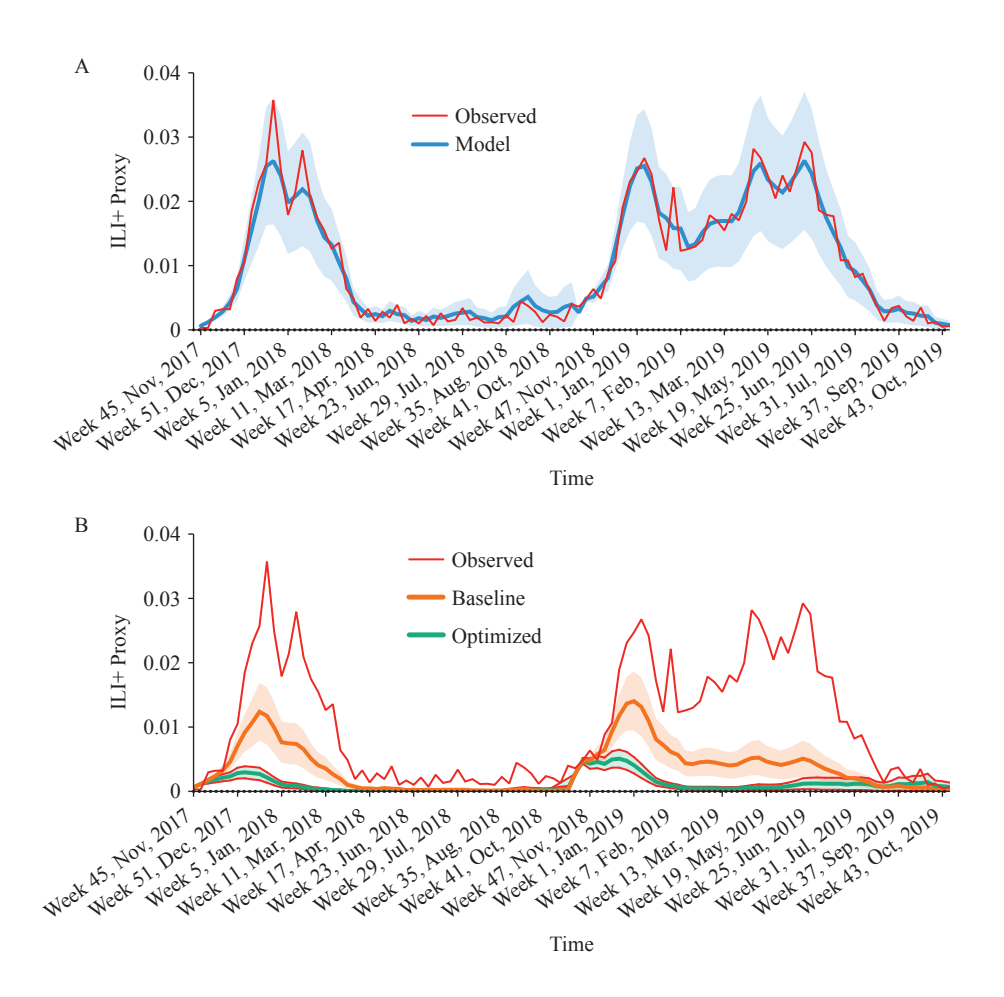


SUPPLEMENTARY FIGURE S2. Schematic representation of the (A) SEYARHD and (B) SEYARHDV epidemiological models for influenza transmission dynamics.

Note: In both frameworks, susceptible individuals transition to an exposed state following infection, where they remain infected but not yet infectious or symptomatic. A proportion of infected cases develop asymptomatic infections with reduced transmissibility before recovering, while the remainder progress to symptomatic illness. Symptomatic individuals subsequently either require hospitalization or recover directly. Hospitalized patients ultimately progress to either recovery or death. Recovered populations gradually return to a susceptible state, maintaining vulnerability to future reinfection. The SEYARHDV model specifically incorporates a vaccinated compartment subdivided into 6 distinct sub-compartments, with protection levels calibrated to estimates reflecting variable vaccine efficacy over time.

Abbreviation: SEYARHD=Susceptible – Exposed – Symptomatic – Asymptomatic – Recovered – Hospitalized – Deceased; SEYARHDV=Susceptible – Exposed – Symptomatic – Asymptomatic – Recovered – Hospitalized – Deceased – Vaccinated.

no symptoms, influenza vaccines may be administered to both susceptible and asymptomatic individuals, though effectiveness is limited to susceptible individuals in preventing infection. $u_{t,a}$ represents the vaccination rate of age group a at time t. β_t indicates the transmission rate at time t, defined as the probability of successful transmission per contact. ϕ_{ai} denotes the average number of contacts an individual in age group a has with age group i. ψ_a represents the population proportion in age group a. ω denotes the relative infectiousness of asymptomatic infections compared to symptomatic infections. σ indicates the proportion of cases that become symptomatic p^{EYA} represents the transition rate from the exposed state; p^{YH} denotes the hospitalization rate of symptomatic cases; p^{YR} , p^{AR} , and p^{HR} represent the recovery rates of symptomatic cases, asymptomatic cases, and hospitalized patients, respectively; p^{HD} represents the mortality rate of hospitalized patients. The specific epidemiological parameter values for the model are presented in Supplementary Table S1.



SUPPLEMENTARY FIGURE S3. Model fitting and simulation of influenza activity under different vaccination strategies, Shenzhen, 2017–2019. (A) Observed ILI+ proxy from surveillance data (red) and corresponding model fitting results (blue line with shaded 95% *CI*). (B) Comparison of observed ILI+ (red) with model-simulated outcomes under two strategies: baseline (orange) and optimized (green), shown as lines with shaded 95% *CIs*.

Note: All scenarios assume identical annual vaccine coverage as implemented in 2023–2024. For school-aged children, only the monthly distribution varies; other age groups maintain actual 2023–2024 vaccination rates. Abbreviation: *CI*=confidence interval; ILI+=influenza-positive proportion.

Ensemble Adjustment Kalman Filter Algorithm

This study employed the highly efficient data assimilation method known as the Ensemble Adjustment Kalman Filter (EAKF) algorithm to estimate weekly transmission rates for historical influenza outbreaks (3–4). The observation and state vectors at time t are denoted as y_t^o and X_p respectively. The state vector is defined as $X_t = (S_{t,1}, E_{t,1}, Y_{t,1}, A_{t,1}, R_{t,1}, H_{t,1}, D_{t,1}, ..., S_{t,4}, E_{t,4}, Y_{t,4}, A_{t,4}, R_{t,4}, H_{t,4}, D_{t,4}, y_p, \beta_t)$, where y_t represents the observed state variable corresponding to symptomatic incidence. In this study's transmission model, weekly symptomatic incidence is calculated as:

$$I_{t} = \sum_{a=1}^{N} \sum_{k=t-6}^{t} \sigma p^{EYA} E_{t,a}$$
 (2)

The EAKF algorithm utilizes an ensemble of particles to represent the posterior distribution of the system state and updates the posterior probability distribution of state X using observations y^o based on Bayesian inference principles. Each particle comprises both a state hypothesis and an associated weight, where the weight indicates the particle's relative contribution to the posterior distribution. During the weight update process, each particle's weight is calculated using a Gaussian likelihood function: $\omega_t^i \propto P(y_t \mid y_t^o, \Omega)$, where $y_t \mid y_t^o$ represents the distance between fitted and observed incidence values, and Ω denotes the variance derived from the standard deviation of the observed incidence vector. These particles undergo resampling according to their weights ω_t^i , which are fitted using

SUPPLEMENTARY TABLE S1. Epidemiological parameters for the influenza transmission model implemented in Shenzhen.

Parameters	Parameter description	Value
N	Total population of Shenzhen	17,681,600 (8)
Ψ	Age-specific population proportions	[0.0566, 0.1314, 0.7584, 0.0535] for [0–5 year, 6–18 year, 19–59 year, ≥60 year] (9)
$\Phi = (\varphi_{ij})$	Contact matrix	[[1.409660734, 1.768548709, 3.751113208, 0.350060933], [0.346000233, 10.64471027, 6.08382839, 0.286702683], [0.570072983, 4.073960628, 10.62071562, 0.482763604], [0.396853292, 1.754034964, 3.745765744, 1.173235326]] for [0–5 year, 6–17 year, 18–59 year, \geq 60 year] (10)
β	Transmission rate	Calibrated
σ	Proportion of infections that are symptomatic	0.55 (11)
ω	Relative infectiousness of asymptomatic infections compared to symptomatic infections	0.36 (11)
p^{RS}	Transition rate from recovered to susceptible state	1/(4×365) (<i>11</i>)
p^{EYA}	Transition rate from exposed to symptomatic/asymptomatic state	1/1.5 (<i>12</i>)
$ ho^{AR}$	Recovery rate of asymptomatic infections	1/3 (13)
p^{YR}	Recovery rate of symptomatic infections	1/5 ×(1-0.0146) (<i>14</i>)
p^{HR}	Recovery rate of hospitalized patients	0.9981 (11)
$ ho^{YH}$	Hospitalization rate	[0.007, 0.0027, 0.0083, 0.0909] for [0–5 year, 6–17 year, 18–59 year, ≥60 year] (11)
$ ho^{\sf HD}$	Case fatality rate among hospitalizations	[0.000050, 0.000072, 0.000595, 0.001570] for [0–5 year, 6–17 year, 18–59 year, \geq 60 year] (11)
u ^A	Annual vaccination coverage rate	[12%, 55%, 12%, 12%] for [0–5 year, 6–18 year, 19–59 year, ≥60 year] (15), with vaccination rates assumed equivalent across all age groups except 6–18 year
V	Vaccine efficacy	$[1/2, 9/10, 7/10, 1/2, 3/10, 1/10]$ for $[V^1, V^2, V^3, V^4, V^5, V^6]$ (2)
f	Transition rate between vaccinated sub-compartments	1/30 (2)
wtp	Willingness of residents to receive influenza vaccines in Shanghai	[0.784, 0.578, 0.730] for [0–18 year, 19–59 year, \ge 60 year] (16)

historical influenza activity data. High-weight particles are retained to ensure that the particle ensemble provides a better approximation of the true posterior distribution.

Retrospective Forecast of Multiple Influenza Seasons

This study reconstructed historical influenza infection patterns in Shenzhen for 2023–2024 using the SEYARHDV model with actual vaccination data incorporated, and for 2017–2019 using the SEYARHD model. During the data assimilation process, we employed Latin Hypercube Sampling (LHS) to draw initial susceptible proportions from a range of [0.65, 0.75], conducting 50 random simulations for each scenario. The weekly incidence rate at time *t*+1 was calculated as the average of these 50 simulation results. In this study, the particle count was set to 10,000. Disease simulations commenced in August (Week 32) for the 2023–2024 period and in November (Week 45) for the 2017–2019 period, approximately one month before the typical onset of each annual influenza season.

Optimization Method

This study integrated a rapid, scalable, and adaptable optimization algorithm with the detailed age-specific influenza transmission model. The time-based intervention policy comprises a sequential series of actions $A_1, A_2, ..., A_T$ implemented over the time span T. The objective involves rapidly searching extensive sets of time-based actions A_i (i.e., vaccination rates implemented at each time step) to identify the most effective policy for achieving public health objectives. In this study, the transmission model returns the cumulative hospitalization incidence throughout the simulation period. To mitigate dispersed vaccination timing and uneven distribution while ensuring policy stability, we introduced a smoothness constraint on the temporal distribution of vaccination coverage, defined as the

sum of squared differences in vaccination rates between consecutive time steps. The optimization function is defined as follows:

$$\min E[\sin(A_1, A_2, \dots, A_T)] + \lambda^* \sum_{i=2, j=i-1}^{T} (A_i - A_j)^2$$
 (3)

where the first term represents the expectation of the stochastic simulation results returned by the transmission model, and the second term constitutes the smoothness regularization term, with $\lambda = 10^{-3}$ representing the regularization coefficient.

To solve this optimization problem, we employed a tree structure to represent all possible strategies. Each tree layer corresponds to a specific time step and contains multiple nodes. Each node connects to multiple edges leading to nodes in the subsequent layer, with each edge representing a possible action at that time step. An intervention strategy is thus mapped to a unique path within the tree structure. To strategically search the tree, we implemented the Upper Confidence Bound Applied to Trees (UCT) algorithm, which selects paths using a multi-armed bandit algorithm within each tree node (5–6). Specifically, suppose we descend the tree to reach a node n connected to k edges representing possible subsequent actions e_1 , e_2 , ..., e_k . Let $N(e_i)$ denote the number of times edge e_i has been selected, and $R(e_i)$ denote the average reward from past simulations that selected edge e_i . The rule for selecting the next edge follows:

$$\arg\max_{i} \left\{ R(e_i) + c \sqrt{\frac{\ln\left(\sum_{i} N(e_i)\right)}{N(e_i)}} \right\} \tag{4}$$

where *c* represents a constant used to balance exploitation and exploration requirements. Through this strategic path sampling approach, well-performing subtrees receive more thorough exploration than those demonstrating poor performance.

Vaccine Administration Settings

The Shenzhen CDC provided vaccination data for school-aged children and other populations in Shenzhen, covering August 2023 to May 2024. Most vaccinations were administered between October and December, achieving an overall population vaccination coverage of 11.91% and a coverage rate of 59.68% among school-aged children. Notably, free, centralized vaccination services are available exclusively to school-aged children in Shenzhen, while individuals in other age groups must voluntarily visit clinics for immunization (7). To estimate vaccination rates for other age groups, we incorporated survey data on adult vaccination willingness following the COVID-19 pandemic in 2020, along with their willingness to vaccinate elderly family members and infants. Based on monthly vaccination rates recorded by the Shenzhen CDC from 2023 to 2024 and vaccination willingness across different age groups, we decomposed the vaccination rates of other populations into age-specific rates to align with the age-group categorization used in the transmission model.

Simulated Epidemiological Impact of Vaccination Strategies on Historical Influenza Outbreaks

This study reconstructed influenza transmission patterns from 2017 to 2019 and conducted a retrospective analysis to simulate the hypothetical outcomes if vaccination strategies had been implemented during this period. The fitting results demonstrate that influenza seasons during these periods spanned approximately from December 2017 to April 2018 and from November 2018 to August 2019 (Supplementary Figure S3A). The second season lasted nearly twice as long as the first, although the peak ILI+ proxy of the first season was slightly higher, with values of 0.0357 in 2017–2018 compared to 0.0293 in 2018–2019. Under the baseline vaccination strategy, where vaccines were distributed evenly across all months, 422,293 (95% CI: 365,424–479,162) symptomatic infections and 17,583 (95% CI: 15,263–19,903) hospitalizations would be averted in 2017–2018, while 841,029 (95% CI: 748,396–933,663) symptomatic infections and 35,543 (95% CI: 31,691–39,395) hospitalizations would be averted in 2018–2019. With the same vaccine supply, the optimized strategy would vaccinate 15% and 45% of school-aged children in October and November, respectively. This strategy could potentially avert 594,234 (95% CI: 517,988–670,480) symptomatic infections and 24,743 (95% CI: 21,621–27,865) hospitalizations in 2017–2018,

and 1,111,011 (95% CI: 988,746–1,233,275) symptomatic infections and 46,918 (95% CI: 41,818–52,019) hospitalizations in 2018–2019. Supplementary Figure S3B further illustrates the differences in ILI+ proxy trends among various vaccination strategies. These results highlight the potential benefits of an optimized vaccination strategy in reducing health burdens. The findings underscore the importance of timing and targeted vaccination, particularly for school-aged children, in mitigating the impact of influenza outbreaks.

Optimized Vaccination Strategies Based on Multi-Year Weighted Evaluation

From a public health perspective, an ideal vaccination strategy must demonstrate consistent robustness across diverse epidemiological scenarios rather than merely excelling in a single year. Given that disease transmission dynamics exhibit annual variation, each year constitutes an independent search scenario, necessitating exploration of a universal optimization strategy that ensures reliable performance across historical periods. While such a strategy may not achieve optimal results in every individual year, it should deliver consistently strong overall performance, thereby establishing a foundation for sustainable, stable, and efficient public health policies. In this study, we conducted five independent optimization searches annually, compiling the results into comprehensive strategy sets. To identify a universal optimal strategy, each candidate strategy was applied across all historical years, with performance evaluated using the objective function. Consequently, the evaluation results for each year required weighting and processing to derive the final optimal strategy Vac*:

$$Vac^* = \arg\min_{Vac \in V} \sum_{y=1}^{Y} w_y H_y^{Vac}$$
 (5)

where Y represents the total number of historical time periods under consideration; V is the feasible set of all possible vaccination strategies. Each strategy $Vac \in V$ is a sequence of actions $Vac = (A1, A2, ..., A_T)$ implemented at each time step t = 1, ..., T; Vac^* denotes the optimal vaccination strategy found by the optimization; H_y^{Vac} represents the proportion of hospitalizations in year y under implementation of strategy Vac. The weight w_y for year y is introduced to adjust for epidemic severity within the objective function and can be defined as follows:

$$w_y = \frac{1}{\text{ILI} + {\text{NoVac} \over y}}$$
 (6)

where ILI+ $_{y}^{\text{NoVac}}$ represents the ILI+ proxy for year y under a no-vaccination scenario.

REFERENCES

- Yang W, Cowling BJ, Lau EHY, Shaman J. Forecasting influenza epidemics in Hong Kong. PLoS Comput Biol 2015;11(7):e1004383. https://doi.org/ 10.1371/journal.pcbi.1004383.
- 2. Doyon-Plourde P, Przepiorkowski J, Young K, Zhao LL, Sinilaite A. Intraseasonal waning immunity of seasonal influenza vaccine a systematic review and meta-analysis. Vaccine 2023;41(31):4462 71. https://doi.org/10.1016/j.vaccine.2023.06.038.
- 3. Yang W, Karspeck A, Shaman J. Comparison of filtering methods for the modeling and retrospective forecasting of influenza epidemics. PLoS Comput Biol 2014;10(4):e1003583. https://doi.org/10.1371/journal.pcbi.1003583.
- Pei S, Teng X, Lewis P, Shaman J. Optimizing respiratory virus surveillance networks using uncertainty propagation. Nat Commun 2021;12(1):222. https://doi.org/10.1038/s41467-020-20399-3.
- 5. Kocsis L, Szepesvári C. Bandit based monte-carlo planning. In: Proceedings of the 17th European conference on machine learning. Berlin, Germany: Springer. 2006; p. 282-93. http://dx.doi.org/10.1007/11871842_29.
- 6. Auer P, Cesa-Bianchi N, Fischer P. Finite-time analysis of the multiarmed bandit problem. Mach Learn 2002;47(2):235 56. https://doi.org/10.1023/A:1013689704352.
- 7. Public Hygiene and Health Commission of Shenzhen Municipality. Flu vaccines have arrived, and these people in Shenzhen will get them for free soon. 2023. https://wjw.sz.gov.cn/ztzl/ymjz/xgzc/content/post_10938913.html. [2024-7-22]. (In Chinese).
- 8. Shenzhen Municipality Bureau of Statistics. Shenzhen Statistical Yearbook 2022. 2023. https://tjj.sz.gov.cn/zwgk/zfxxgkml/tjsj/tjnj/content/post_10390917.html. [2024-5-15]. (In Chinese)
- 9. Shenzhen Municipality Bureau of Statistics. The Seventh National Population Census of Shenzhen. 2022. https://tjj.sz.gov.cn/ztzl/zt/szsdqcqgrkpc/. [2024-2-8]. (In Chinese)
- 10. Mistry D, Litvinova M, Pastore Y Piontti A, Chinazzi M, Fumanelli L, Gomes MFC, et al. Inferring high-resolution human mixing patterns for disease modeling. Nat Commun 2021;12(1):323. https://doi.org/10.1038/s41467-020-20544-y.
- 11. Du ZW, Fox SJ, Ingle T, Pignone MP, Meyers LA. Projecting the combined health care burden of seasonal influenza and COVID-19 in the 2020-2021 season. MDM Policy Pract 2022;7(1):23814683221084631. http://dx.doi.org/10.1177/23814683221084631.
- 12. Boëlle PY, Ansart S, Cori A, Valleron AJ. Transmission parameters of the A/H1N1 (2009) influenza virus pandemic: a review. Influenza Other Respir Viruses 2011;5(5):306 16. https://doi.org/10.1111/j.1750-2659.2011.00234.x.
- 13. Wu JT, Leung GM, Lipsitch M, Cooper BS, Riley S. Hedging against antiviral resistance during the next influenza pandemic using small stockpiles of

China CDC Weekly

- an alternative chemotherapy. PLoS Med 2009;6(5):e1000085. https://doi.org/10.1371/journal.pmed.1000085.
- 14. Yang Y, Sugimoto JD, Halloran ME, Basta NE, Chao DL, Matrajt L, et al. The transmissibility and control of pandemic influenza A (H1N1) virus. Science 2009;326(5953):729 33. https://doi.org/10.1126/science.1177373.
- 15. Chen DQ, Jiang YW, Huang F, Wu XL, Ye ZJ, Wu Y, et al. Effectiveness of influenza vaccination for school-age children in preventing school absenteeism in Shenzhen: an empirical study. Chin J Epidemiol 2021;42(10):1900 6. https://doi.org/10.3760/cma.j.cn112338-20210723-00580.
- Zhou YH, Tang J, Zhang JJ, Wu QS. Impact of the coronavirus disease 2019 epidemic and a free influenza vaccine strategy on the willingness of residents to receive influenza vaccines in Shanghai, China. Hum Vaccin Immunother 2021;17(7):2289 92. https://doi.org/10.1080/21645515.2020. 1871571.